WIRELESS LOCATION TRACKING VIA COMPLEX-DOMAIN SUPER MDS WITH TIME SERIES SELF-LOCALIZATION INFORMATION

Yuya Nishi[1], *Takumi Takahashi*[1], *Hiroki Iimori*[2], *Giuseppe Abreu*[3], *Shinsuke Ibi*[4], *and Seiichi Sampei*[1]

[1]Graduate School of Engineering, Osaka University, [2]Ericsson Research,
[3]School of Computer Science and Engineering, Jacobs University Bremen,
[4]Faculty of Science and Engineering, Doshisha University

ABSTRACT

We propose a wireless localization algorithm based on complex-domain super multidimensional scaling (CD-SMDS) augmented with a self-localization (SL) component, whereby each target tracks its own motion by incorporating bearing information, obtained $e.g.$, from integrated inertial sensors. The proposed method improves localization accuracy by simultaneously using the time series information of distance and angle associated to the SL information in order to construct the SMDS rank-one edge kernel matrix, maximizing the noise reduction effect of the low-rank truncation via singular value decomposition (SVD). The efficacy of the proposed method over the original CD-SMDS is confirmed via software simulations, and compared with an SL-aware Cramér-Rao lower bound (CRLB).

***Index Terms*—** Wireless indoor localization, multidimensional scaling, time series information

1. INTRODUCTION

With the penetration of wireless communication networks into new and diverse areas of applications [1, 2, 3], the importance of location information in modern systems is approaching that of communication payload data. In particular, internet of things (IoT) applications [4] often rely on networks consisting of large numbers of nodes typically limited in computational capabilities [5, 6], such that low-complexity localization algorithms based on multidimensional information aggregated from the nodes are of interest.

Within this context, we investigate an improved low-complexity algorithm based on the isometric embedding technique, also known as multidimensional scaling (MDS) [7, 8], which possesses a well-determined computational complexity, unlike the approaches based on Bayesian [9] and convex optimization [10]. To name a few recent MDS-based localization algorithms, the super MDS (SMDS) framework of [11, 12] can handle hybrid information ($i.e.$, both distance and angle) simultaneously, and was shown to significantly outperform the classic MDS technique even under uncertainties in the angle domain in the order of $\pm 35^\circ$. In [13], a complex-domain SMDS (CD-SMDS) was proposed which achieves further complexity reduction and accuracy improvement via the elimination of redundancy resulting from casting the latter SMDS algorithm onto the complex domain.

The improvement of CD-SMDS over real-valued SMDS is due to a noise reduction effect of the low-rank truncation via singular value decomposition (SVD) of the edge kernel matrix, which in the case of the CD-SMDS algorithm has rank one, which suggests that further improvement can be expected in systems of larger dimensions. Indeed, MDS algorithms are typically limited to snapshot positioning ($i.e.$, location inference based on observations from a single time slot), leaving potential for improvement in the context of tracking systems, whereby the temporal dimension is also incorporated. To this end, we further extend the original CD-SMDS framework such that further noise reduction effects can be obtained by exploiting time series information.

With the recent development of multifunctional sensor devices, target devices can easily estimate the distance and direction of their own movement using a set of low-cost inertial sensors [14, 15]. Such inertial information between certain time slots obtained from the self-localization (SL) enables us to bridge the information at time slot t with the information at the previous discrete time slot ($i.e.$, $t-1$), and to boost localization accuracy by constructing a larger rank-one edge kernel matrix in the MDS framework, encompassing the time series information of both distance and angle. In addition, the algorithm design along with the CD-SMDS framework allows us to analyze the achievable performance of the proposed method in terms of the Cramér-Rao lower bound (CRLB), taking into account the error of SL.

Notation: Vectors and matrices are denoted by lower- and upper-case bold-face letters, respectively. The conjugate, transpose, and conjugate transpose operators are denoted by $\cdot^*$, $\cdot^\mathsf{T}$, and $\cdot^\mathsf{H}$. Imaginary units are denoted by $\mathrm{j} = \sqrt{-1}$, real numbers of size $a \times b$ are denoted by $\mathbb{R}^{a\times b}$ and complex numbers by $\mathbb{C}^{a\times b}$. The $a\times a$ square identity matrix is denoted by $\boldsymbol{I}_a$. The $a\times b$ zero matrix is denoted by $\mathbf{0}_{a\times b}$ and the $a\times b$ one matrix is denoted by $\mathbf{1}_{a\times b}$. $\mathrm{diag}\,(\boldsymbol{a})$ denotes a diagonal matrix whose main diagonal is $\boldsymbol{a}$. $\|\cdot\|$ denotes the Euclidean norm. $\langle\cdot,\cdot\rangle$ and $|\cdot\times\cdot|$ denote the inner product and the outer product, respectively. $\det(\boldsymbol{A})$ denotes the determinant of $\boldsymbol{A}$.

2. FULL CD-SMDS ALGORITHM

Consider a localization network in a 2-dimensional Euclidean space containing N nodes, out of which N_A nodes are referred to as anchor nodes (ANs) with their locations known a priori, while the location of the remaining $N_\mathrm{T} \triangleq N - N_\mathrm{A}$

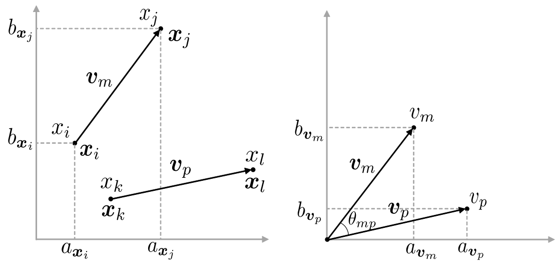

(a) Vertices (b) Edges

Fig. 1. Illustration of vector and complex representation of vertices and edges of a network

nodes, hereafter referred to as target nodes (TNs), is to be estimated based on measurements of their mutual distances and angles [12]. Let the coordinates of the i-th node be denoted by the column vector $\boldsymbol{x}_i = [a_{\boldsymbol{x}_i}, b_{\boldsymbol{x}_i}]^\mathsf{T} \in \mathbb{R}^{2\times 1}$, such that the coordinates of all nodes in the network can be arranged in the coordinate matrix

$$\boldsymbol{X} \triangleq [\boldsymbol{x}_1, \ldots, \boldsymbol{x}_N]^\mathsf{T} \in \mathbb{R}^{N\times 2}. \tag{1}$$

Consider the set of unique index pairs $\mathcal{M} \triangleq \{(1,2), \cdots, (1,N), (2,3), \cdots, (N-1,N)\}$ in an ascending order, such that each pair $m \in \mathcal{M}$ corresponds to an edge vector $\boldsymbol{v}_m$ in the form of

$$\boldsymbol{v}_m = \boldsymbol{x}_i - \boldsymbol{x}_j, \quad j > i, \tag{2}$$

where the Euclidean distance between the corresponding pair is simply given by $d_m \triangleq \|\boldsymbol{v}_m\|$.

As shown in [13], the full CD-SMDS algorithm proposed to convert the above expressions to its complex counterpart; in other words, the coordinate vector $\boldsymbol{x}_i \in \mathbb{R}^{2\times 1}$ of a generic node i in the network can be alternatively expressed by the complex representation $\boldsymbol{x}_i \in \mathbb{R}^2$, *i.e.,*

$$\boldsymbol{x}_i \triangleq [a_{\boldsymbol{x}_i}, b_{\boldsymbol{x}_i}]^\mathsf{T} \Longleftrightarrow x_i \triangleq a_{\boldsymbol{x}_i} + \mathrm{j} b_{\boldsymbol{x}_i}, \tag{3}$$

and the complex coordinate vector is given by

$$\boldsymbol{x} \triangleq [x_1, \ldots, x_N]^\mathsf{T} \in \mathbb{C}^{N\times 1}. \tag{4}$$

Similarly, the edge vector $\boldsymbol{v}_m$ between any two nodes $\boldsymbol{x}_i$ and $\boldsymbol{x}_j$ can be represented as

$$\boldsymbol{v}_m \Longleftrightarrow v_m = a_{\boldsymbol{v}_m} + \mathrm{j} b_{\boldsymbol{v}_m}, \quad j > i, \tag{5}$$

where $a_{\boldsymbol{v}_m} \triangleq a_{\boldsymbol{x}_j} - a_{\boldsymbol{x}_i}$, $b_{\boldsymbol{v}_m} \triangleq b_{\boldsymbol{x}_j} - b_{\boldsymbol{x}_i}$, and the amplitude of v_m is given by $|v_m| \triangleq d_m = \sqrt{a^2_{\boldsymbol{v}_m} + b^2_{\boldsymbol{v}_m}}$.

From the above, the complex edge matrix consisting of the collection of all $M \triangleq \binom{N}{2} = N(N-1)/2$ edge vectors can be concisely written as

$$\begin{aligned} \boldsymbol{v} &\triangleq [(x_1 - x_2), (x_1 - x_3), \ldots, (x_{N-1} - x_N)]^\mathsf{T} \\ &= [v_1, \ldots, v_M]^\mathsf{T} = \boldsymbol{C} \cdot \boldsymbol{x} \in \mathbb{C}^{M\times 1}, \end{aligned} \tag{6}$$

where

$$\boldsymbol{C} \triangleq \left[\begin{array}{c|c|c|c} \boldsymbol{1}_{N-1\times 1} & \multicolumn{3}{c}{-\boldsymbol{I}_{N-1}} \\ \hline \boldsymbol{0}_{N-2\times 1} & \boldsymbol{1}_{N-2\times 1} & \multicolumn{2}{c}{-\boldsymbol{I}_{N-2}} \\ \hline \multicolumn{2}{c|}{\ddots} & \ddots & \ddots \\ \hline \multicolumn{3}{c|}{\boldsymbol{0}_{1\times N-2}} & 1 \mid -1 \end{array}\right] \in \mathbb{R}^{M\times N}. \tag{7}$$

Using the fact that the inner and outer products between the edge vectors $\boldsymbol{v}_m$ and $\boldsymbol{v}_p$ are respectively given by

$$\langle \boldsymbol{v}_m, \boldsymbol{v}_p \rangle = a_{\boldsymbol{v}_m} a_{\boldsymbol{v}_p} + b_{\boldsymbol{v}_m} b_{\boldsymbol{v}_p} = d_m d_p \cos\theta_{mp}, \tag{8a}$$

$$|\boldsymbol{v}_m \times \boldsymbol{v}_p| = a_{\boldsymbol{v}_m} b_{\boldsymbol{v}_p} - a_{\boldsymbol{v}_p} b_{\boldsymbol{v}_m} = d_m d_p \sin\theta_{mp}, \tag{8b}$$

the product of a pair of edge vectors $\boldsymbol{v}_m$ and $\boldsymbol{v}_p^*$ with $m \neq p$ is given by

$$v_m \cdot v_p^* = d_m d_p \left(\cos\theta_{mp} + \mathrm{j}\sin\theta_{mp}\right) = d_m d_p e^{\mathrm{j}\theta_{mp}}, \tag{9}$$

where θ_{mp} is the difference in phase.

Based on the above, the complex-domain edge kernel matrix $\boldsymbol{K}$ that includes all distance and phase difference information can be expressed as [13]

$$\boldsymbol{K} \triangleq \boldsymbol{v} \cdot \boldsymbol{v}^\mathsf{H} = \mathrm{diag}(\boldsymbol{d}) \cdot \begin{bmatrix} e^{\mathrm{j}\theta_{11}} & \cdots & e^{\mathrm{j}\theta_{1M}} \\ \vdots & \ddots & \vdots \\ e^{\mathrm{j}\theta_{M1}} & \cdots & e^{\mathrm{j}\theta_{MM}} \end{bmatrix} \cdot \mathrm{diag}(\boldsymbol{d}), \tag{10}$$

where $\boldsymbol{d} \triangleq [d_1, \ldots, d_M]^\mathsf{T}$.

From (10), it is evident that an edge kernel matrix $\tilde{\boldsymbol{K}}$ of rank 1 can be obtained from distance and phase measurements $\tilde{d}_m$ and $\tilde{\theta}_{mp}$, and therefore the estimate of $\boldsymbol{v}$ is given by

$$\hat{\boldsymbol{v}} = \sqrt{\lambda}\boldsymbol{u}, \tag{11}$$

where $(\lambda, \boldsymbol{u})$ is the dominant eigenpair of $\tilde{\boldsymbol{K}}$.

Finally, the estimate coordinate vector $\hat{\boldsymbol{x}}$ can be recovered from $\hat{\boldsymbol{v}}$ by inverting the relationship in equation (6), *i.e.,*

$$\left[\begin{array}{c} \boldsymbol{x}_\mathrm{A} \\ \hline \hat{\boldsymbol{x}} \end{array}\right] = \left[\begin{array}{c|c} \boldsymbol{I}_{N_\mathrm{A}} & \boldsymbol{0}_{N_\mathrm{A}\times N_\mathrm{T}} \\ \hline \multicolumn{2}{c}{\boldsymbol{C}} \end{array}\right]^{-1} \cdot \left[\begin{array}{c} \boldsymbol{x}_\mathrm{A} \\ \hline \hat{\boldsymbol{v}} \end{array}\right], \tag{12}$$

where the vector consisting of the complex coordinates of ANs $\boldsymbol{x}_\mathrm{A} \in \mathbb{C}^{N_\mathrm{A}\times 1}$ is used to circumvent the rank-deficient problem of the matrix $\boldsymbol{C}$. Furthermore, a Procrustes transformation [16] may be required to bring the resulting estimate $\hat{\boldsymbol{x}}$ to the same scale, orientation, and coordinate origin of the true coordinates $\boldsymbol{x}$. Besides the above concise description of CD-SMDS, we refer the reader to [12] for more detailed information.

3. FULL SL-CD-SMDS ALGORITHM

Extending snapshot-based CD-SMDS to a location tracking algorithm with multiple targets [17], this section presents the proposed SL-aided CD-SMDS (SL-CD-SMDS) algorithm that takes into account measurements from two consecutive time slots by seamlessly integrating available coordinate information. To that end, let the part of edge vector $\boldsymbol{v}$ in equation (6) corresponding to edges between ANs, the part corresponding to edges between ANs and TNs, and the part corresponding to edges between TNs be $\boldsymbol{v}_\mathrm{AA}$, $\boldsymbol{v}_\mathrm{AT}$, and $\boldsymbol{v}_\mathrm{TT}$, respectively. Defining the vector consisting of the complex coordinates of TNs at discrete time slot t as $\boldsymbol{x}_\mathrm{T}^{(t)} \in \mathbb{C}^{N_\mathrm{T}\times 1}$, the *extended* complex coordinate vector including the coordinates of TNs at $t-1$ is defined as

$$\boldsymbol{x}' \triangleq \left[\boldsymbol{x}_\mathrm{A}^\mathsf{T} \quad \left(\boldsymbol{x}_\mathrm{T}^{(t-1)}\right)^\mathsf{T} \quad \left(\boldsymbol{x}_\mathrm{T}^{(t)}\right)^\mathsf{T}\right]^\mathsf{T} \in \mathbb{C}^{(N+N_\mathrm{T})\times 1}, \tag{13}$$

where $\boldsymbol{x}_\mathrm{T}^{(t-1)}$ is a location estimate from SL and therefore known at time t such that $\boldsymbol{x}_\mathrm{T}^{(t-1)}$ can be seen as ANs with position errors and uncertainties.

With that in mind, the complex edge vector between ANs can be expressed as

$$\boldsymbol{v}_{\mathrm{AA}} = \boldsymbol{C}_{\mathrm{AA}} \cdot \boldsymbol{x}', \tag{14}$$

where $\boldsymbol{C}_{\mathrm{AA}} \in \mathbb{R}^{M \times (N+N_{\mathrm{T}})}$ is defined as

$$\boldsymbol{C}_{\mathrm{AA}} \triangleq \left[\begin{array}{c|c|c|c|c}
\mathbf{1}_{N-1\times 1} & \multicolumn{3}{c|}{-\boldsymbol{I}_{N-1}} & \mathbf{0}_{N-1\times N_{\mathrm{T}}} \\ \hline
\mathbf{0}_{N-2\times 1} & \mathbf{1}_{N-2\times 1} & \multicolumn{2}{c|}{-\boldsymbol{I}_{N-2}} & \mathbf{0}_{N-2\times N_{\mathrm{T}}} \\ \hline
\multicolumn{2}{c|}{\ddots} & \ddots & \ddots & \vdots \\ \hline
\multicolumn{2}{c|}{\mathbf{0}_{1\times N-2}} & 1 & -1 & \mathbf{0}_{1\times N_{\mathrm{T}}}
\end{array}\right]. \tag{15}$$

Unlike CD-SMDS, the complex edge vector $\boldsymbol{v}_{\mathrm{AT}}$ is now composed of two different edge vectors, *i.e.,* 1) the edges between $\boldsymbol{x}_{\mathrm{A}}$ and $\boldsymbol{x}_{\mathrm{T}}^{(t)}$, and 2) the edges between $\boldsymbol{x}_{\mathrm{T}}^{(t-1)}$ and $\boldsymbol{x}_{\mathrm{T}}^{(t)}$. For the edge kernel matrix corresponding to 2), only the part corresponding to their own movements that can be informed by SL can be constructed. These edges bridge the information of different discrete time slots and provides an improvement over the original CD-SMDS based on the snapshot approach. Accordingly, $\boldsymbol{v}_{\mathrm{AT}}$ is given by

$$\boldsymbol{v}_{\mathrm{AT}} = \boldsymbol{C}_{\mathrm{AT}} \cdot \boldsymbol{x}', \tag{16}$$

where $\boldsymbol{C}_{\mathrm{AT}} \in \mathbb{R}^{N_{\mathrm{T}}(N_{\mathrm{A}}+1) \times (N+N_{\mathrm{T}})}$ is defined as

$$\boldsymbol{C}_{\mathrm{AT}} \triangleq \left[\begin{array}{c|c|c|c|c}
\mathbf{1}_{N_{\mathrm{T}}\times 1} & \multicolumn{3}{c|}{\mathbf{0}_{N_{\mathrm{T}}\times N-1}} & -\boldsymbol{I}_{N_{\mathrm{T}}} \\ \hline
\mathbf{0}_{N_{\mathrm{T}}\times 1} & \mathbf{1}_{N_{\mathrm{T}}\times 1} & \multicolumn{2}{c|}{\mathbf{0}_{N_{\mathrm{T}}\times N-2}} & -\boldsymbol{I}_{N_{\mathrm{T}}} \\ \hline
\ddots & \ddots & \multicolumn{2}{c|}{\ddots} & \vdots \\ \hline
\multicolumn{2}{c|}{\mathbf{0}_{N_{\mathrm{T}}\times N_{\mathrm{A}}-1}} & \mathbf{1}_{N_{\mathrm{T}}\times 1} & \mathbf{0}_{N_{\mathrm{T}}\times N_{\mathrm{T}}} & -\boldsymbol{I}_{N_{\mathrm{T}}} \\ \hline
\multicolumn{3}{c|}{\mathbf{0}_{N_{\mathrm{T}}\times N_{\mathrm{A}}}} & \boldsymbol{I}_{N_{\mathrm{T}}} & -\boldsymbol{I}_{N_{\mathrm{T}}}
\end{array}\right]. \tag{17}$$

Similarly, the complex edge vector corresponding to the TNs (*i.e.,* $\boldsymbol{v}_{\mathrm{TT}}$) is given by

$$\boldsymbol{v}_{\mathrm{TT}} = \boldsymbol{C}_{\mathrm{TT}} \cdot \boldsymbol{x}', \tag{18}$$

where $\boldsymbol{C}_{\mathrm{TT}} \in \mathbb{R}^{N_{\mathrm{T}}(N_{\mathrm{T}}-1)/2 \times (N+N_{\mathrm{T}})}$ is defined as

$$\boldsymbol{C}_{\mathrm{TT}} \triangleq \left[\begin{array}{c|c|c|c|c}
\mathbf{0}_{N_{\mathrm{T}}-1\times N} & \mathbf{1}_{N_{\mathrm{T}}-1\times 1} & \multicolumn{3}{c}{-\boldsymbol{I}_{N_{\mathrm{T}}-1}} \\ \hline
\mathbf{0}_{N_{\mathrm{T}}-2\times N} & \mathbf{0}_{N_{\mathrm{T}}-2\times 1} & \mathbf{1}_{N_{\mathrm{T}}-2\times 1} & \multicolumn{2}{c}{-\boldsymbol{I}_{N_{\mathrm{T}}-2}} \\ \hline
\vdots & \ddots & \ddots & \multicolumn{2}{c}{\ddots} \\ \hline
\mathbf{0}_{1\times N} & \multicolumn{2}{c|}{\mathbf{0}_{1\times N_{\mathrm{T}}-2}} & 1 & -1
\end{array}\right]. \tag{19}$$

Given the complex edge vectors in equations (14), (16), and (18), a new complex-domain edge kernel matrix that integrates the time series information of distance and angle can be expressed as

$$\boldsymbol{K}' \triangleq \boldsymbol{v}' \cdot \boldsymbol{v}'^{\mathsf{H}}, \tag{20}$$

where

$$\boldsymbol{v}' \triangleq \begin{bmatrix} \boldsymbol{v}_{\mathrm{AA}}^{\mathsf{T}} & \boldsymbol{v}_{\mathrm{AT}}^{\mathsf{T}} & \boldsymbol{v}_{\mathrm{TT}}^{\mathsf{T}} \end{bmatrix}^{\mathsf{T}} = \boldsymbol{C}' \cdot \boldsymbol{x}' \in \mathbb{C}^{M' \times 1}, \tag{21a}$$

$$\boldsymbol{C}' \triangleq \begin{bmatrix} \boldsymbol{C}_{\mathrm{AA}}^{\mathsf{T}} & \boldsymbol{C}_{\mathrm{AT}}^{\mathsf{T}} & \boldsymbol{C}_{\mathrm{TT}}^{\mathsf{T}} \end{bmatrix}^{\mathsf{T}} \in \mathbb{R}^{M' \times (N+N_{\mathrm{T}})}, \tag{21b}$$

and $M' \triangleq \binom{N+N_{\mathrm{T}}}{2} - N_{\mathrm{T}}(N_{\mathrm{T}}-1)$.

With the extended edge kernel matrix $\tilde{\boldsymbol{K}}'$ given in (20), an estimate of the coordinates can be obtained by following the CD-SMDS procedure as in (11) and (12).

Algorithm 1 Full SL-CD-SMDS ($t \geq 2$)

Input:
- *Measurements of distance and angles:* $\tilde{d}_m$ *and* $\tilde{\theta}_{mp}$.
- *Measurements* $\tilde{d}_m$ *and* $\tilde{\theta}_m$ *from SL*

Steps:
- *Estimate the complex edge vector* $\boldsymbol{v}_{AA}$ *using* (14)
- *Use* $\tilde{d}_m$, $\tilde{\theta}_{mp}$, $\tilde{\theta}_m$, *and* $\boldsymbol{v}_{AA}$ *to construct* $\tilde{\boldsymbol{K}}'$ *as in* (20)
- *Compute the largest eigenpair* $(\lambda, \boldsymbol{u})$ *of* $\tilde{\boldsymbol{K}}'$.
- *Estimate the complex edge vector* $\hat{\mathbf{v}}$ *using* (11)
- *Compute* $\hat{\boldsymbol{x}}'$ *by inversion using* (21a)
- *Map* $\hat{\boldsymbol{x}}'$ *back to* $\hat{\boldsymbol{X}}$ *and apply Procrustes if needed*

Since the size of the kernel matrix increases from $M \times M$ of CD-SMDS to $M' \times M'$, localization performance improvements can be expected due to further noise suppression via the low-rank truncation performed in (11). For the sake of completeness, we conclude this section with a pseudo-code of the SL-CD-SMDS algorithm, which is offered in Algorithm 1.

Thecomputationalcomplexity of SL-CD-SMDS is $\mathcal{O}(M'^2)$; however, it is not expected to lead to severe delays, since efficient subspace tracking algorithms can reduce the complexity required for SVD at each time slot [18].

4. SIMULATION RESULT

Computer simulations were conducted to validate the performance of the proposed SL-CD-SMDS algorithm. The simulation is performed with the test area of 10 [m]-by-10 [m] equipped with 4 ANs, one at each corner, and populated with N_{T} TNs located randomly in its interior with x and y coordinates following a uniform distribution. The TNs follow independent random trajectories generated accordingly to a first-order autoregressive (AR) model [17]. Distance measurements are modeled as gamma-distributed random variables [19] with the mean given by the true distance d and a standard deviation σ_d. The probability density function (PDF) of measured distances $\tilde{d}$ associated with d is given by

$$p\left(d; \alpha, \beta\right) = \left(\beta^{\alpha}\Gamma(\alpha)\right)^{-1} \cdot \tilde{d}^{(\alpha-1)} \cdot e^{\tilde{d}/\beta}, \tag{22}$$

where $\alpha \triangleq d^2/\sigma_d^2$ and $\beta \triangleq \sigma_d^2/d$.

In turn, angle measurement errors δ_θ are assumed to be Tikhonov-distributed [20, 21]. The PDF of measured angles $\tilde{\theta} = \theta + \delta_\theta$ associated with a true angle θ is given by

$$p\left(\tilde{\theta}; \theta, \rho\right) = \left(2\pi I_0(\rho)\right)^{-1} \cdot \exp\left[\rho\cos(\theta - \tilde{\theta})\right], \tag{23}$$

where the concentration parameter $\rho \geq 0$ is inversely proportional to the angular error variance. Due to the non-linear relationship between angular error variances and ρ, the influence of angular errors by the quantity ϵ_θ, defined as the bounding angle of the 90[th] centered percentile, is captured by

$$\epsilon_\theta = \theta_{\mathrm{B}} \Big| \int_{-\theta_{\mathrm{B}}}^{\theta_{\mathrm{B}}} p_{\Theta}(\phi; 0, \rho) d\phi = 0.9. \tag{24}$$

It is assumed that SL is also subject to measurement errors by equations (22)-(24). Estimation errors are measured by the Frobenius norm of the difference between the estimates $\hat{\mathbf{X}}$ and true TNs' positions $\mathbf{X}$, *i.e.* mean square error (MSE), $\xi = \frac{1}{N_t}\|\hat{\mathbf{X}} - \mathbf{X}\|_{\mathrm{F}}$, where $\|\cdot\|_{\mathrm{F}}$ denotes the Frobenius norm.

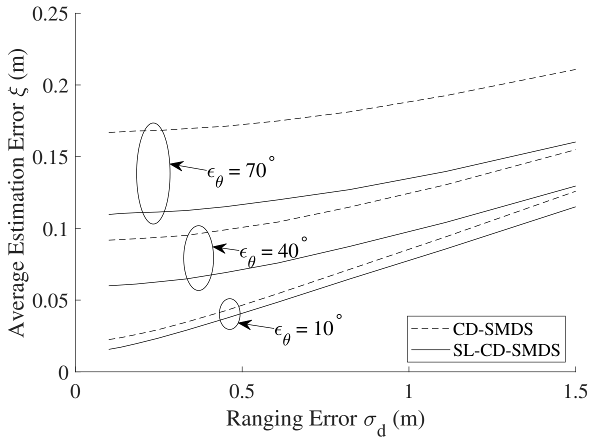

Fig. 2. Localization accuracies v.s. ranging errors ($N_{\mathrm{T}} = 6$)

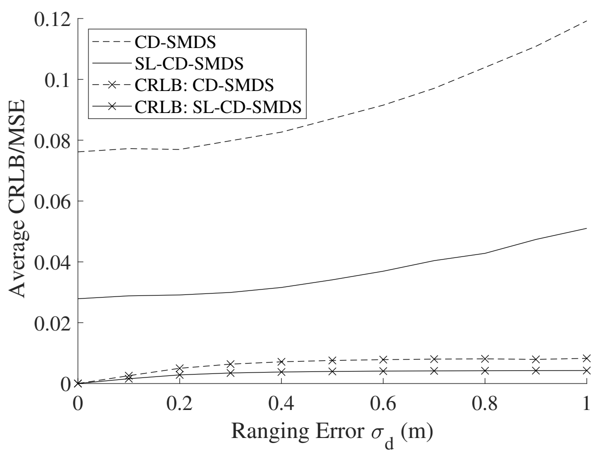

Fig. 3. Average MSE v.s. ranging errors ($N_{\mathrm{T}} = 6$)

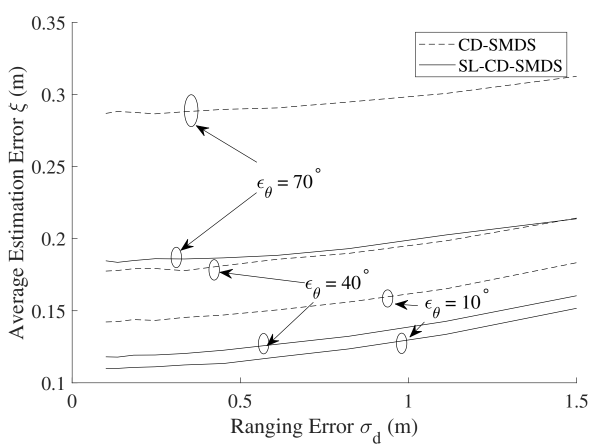

Fig. 4. Localization accuracies v.s. ranging errors ($N_{\mathrm{T}} = 6$)

Fig. 2 compares the localization accuracy of the CD-SMDS and SL-CD-SMDS algorithms for $N_{\mathrm{T}} = 6$ as a function of the standard deviations of Gamma-distributed distance estimates, where three different levels of Tikhonov-distributed angle estimation errors are considered. It is found that the proposed method outperforms the original CD-SMDS algorithm over a wide range of ranging errors due to the improved noise suppression effect resulting from the extended edge kernel matrix. One can also perceive that the gain in comparison with CD-SMDS increases as the angle estimation error level grows, the reason for which can be attributed to the enhanced noise suppression of the proposed SL-CD-SMDS.

Fig. 3 shows the MSE performances for $\epsilon_\theta = 10°$ and $N_{\mathrm{T}} = 6$ as a function of the standard deviations of Gamma-distributed distance estimates. The proposed method significantly outperforms the CD-SMDS algorithm. To clarify the performance limit, the CRLB [22] is also presented, which is computed based on the measurement method and the distribution of measurement errors. As described above, the distance errors follow the gamma distribution and the angle errors follow the Tikhonov distribution. Distance measurements are performed by time of arrival (ToA) [23] for both $\boldsymbol{v}_{\mathrm{AT}}$ and $\boldsymbol{v}_{\mathrm{TT}}$, and angle measurements are performed by angle of arrival (AoA) [24] for $\boldsymbol{v}_{\mathrm{AT}}$ and by angle difference of arrival (ADoA) [25] for $\boldsymbol{v}_{\mathrm{TT}}$. Under the assumption that the uncertainty of $\boldsymbol{x}_{\mathrm{T}}^{(t-1)}$ is relatively small compared to the ranging errors, the CRLB of SL-CD-SMDS can be derived using the analytical framework presented in [26], taking into account the estimation errors at $t-1$. The lower bound of the proposed method is found to be below the conventional one.

Finally, we now turn our attention to more practical cases where distance and angle information between nodes was partially unattainable, *e.g.*, due to non-line of sight (NLoS) environments between nodes. Fig. 4 shows the performances of CD-SMDS and SL-CD-SMDS for a case where 40% of the entries in the kernels $\boldsymbol{K}$ and $\boldsymbol{K}'$ are randomly erased. To obtain the final results shown in the plots, the randomly (but identically) erased kernels are first complemented using the low-rank matrix completion method [27] before running the localization algorithms, and averaged over multiple independent erasure realizations. While observation incompleteness clearly affects the performance from a comparison with Fig. 2, the proposed SL-CD-SMDS is more robust against erasure than the original CD-SMDS, which is again explained by information complemented by a larger dimension size of $\boldsymbol{K}'$ and the improved noise suppression effect.

5. CONCLUSION

In this paper, we proposed a novel wireless location tracking algorithm dubbed the SL-CD-SMDS, which is an extension of the state-of-the-art CD-SMDS to location tracking problems under the assumption that time series information of distance and angle simultaneously can be utilized. The resulting high-dimensional edge kernel matrix effectively separates the signal and noise spaces, maximizing the benefit of noise reduction performed by the low-rank truncation via SVD. Simulation results show that the proposed method significantly outperforms the conventional method, especially when the measurement error is large. In addition, the CRLB of the proposed method is presented to clarify the performance limit.

6. ACKNOWLEDGMENT

A part of this research was supported by JSPS KAKENHI Grant Number JP22H01483.

7. REFERENCES

[1] H. Chen et al., "A tutorial on terahertz-band localization for 6G communication systems," *IEEE Commun. Survey Tut.*, vol. 24, no. 3, pp. 1780–1815, 2022.

[2] P. K. R. Maddikunta et al., "Industry 5.0: A survey on enabling technologies and potential applications," *J. Ind. Inf. Integr.*, vol. 26, pp. 100257, 2022.

[3] T. Savić, X. Vilajosana, and T. Watteyne, "Constrained localization: A survey," *IEEE Access*, vol. 10, pp. 49297–49321, 2022.

[4] M. Wollschläger, T. Sauter, and J. Jasperneite, "The future of industrial communication: Automation networks in the era of the internet of things and industry 4.0," in *IEEE Ind. Electron. Mag*, Oct 2017, vol. 11, pp. 17–27.

[5] H. Wymeersch and G. Seco-Granados, "Radio localization and sensing – Part II: State-of-the-art and challenges," *IEEE Commun. Lett.*, 2022.

[6] J. Xiao et al., "A survey on wireless indoor localization from the device perspective," *ACM Comput. Surv.*, vol. 49, no. 2, pp. 1–31, jun 2016.

[7] W. S. Torgerson, "Multidimensional scaling: I. theory and method," *IEEE Trans. Signal Processing*, vol. 17, no. 4, pp. 401–419, 1952.

[8] T. F. Cox and M. A. A. Cox, *Multidimensional Scaling*, 2nd ed. London,U.K.: Chapman & Hall, 2000.

[9] ÁF. Garcia-Fernandez, L. Svensson, and S. Särkkä, "Cooperative localization using posterior linearization belief propagation," *IEEE Trans. Vehicular Technology*, vol. 67, no. 1, pp. 832–836, 2018.

[10] X. Shi et al., "Robust localization using range measurements with unknown and bounded errors," *IEEE Trans. Wireless Commun.*, vol. 16, no. 6, pp. 4065–4078, 2017.

[11] D. Macagnano and G. T. F. de Abreu, "Algebraic approach for robust localization with heterogeneous information," in *IEEE Trans. Wireless Commun*, Oct 2013, vol. 12, p. 5334–5345.

[12] G. T. F. de Abreu and G. Destino, "Super MDS: Source location from distance and angle information," in *in Proc. IEEE Wireless Commun. Netw. Conf. (WCNC)*, Mar 2007, vol. 2, p. 4430–4434.

[13] A. Ghods and G. T. F. de Abreu, "Complex-domain super MDS: A new framework for wireless localization with hybrid information," *IEEE Trans. Wireless Commun.*, vol. 17, no. 11, pp. 7364–7378, 2018.

[14] M. Kok, J. D. Hol, and T. B. Schön, *Using Inertial Sensors for Position and Orientation Estimation*, Now Foundations and Trends, 2017.

[15] S. V. de Velde, G. T. F. de Abreu, and H. Steendam, "Improved censoring and NLOS avoidance for wireless localization in dense networks," *IEEE J. Sel. Areas in Commun.*, vol. 33, no. 11, pp. 2302–2312, 2015.

[16] P.D. Fiore, "Efficient linear solution of exterior orientation," in *IEEE Commun. Surveys Tuts*, Feb 2001, vol. 23, pp. 140–148.

[17] D. Macagnano and G. T. F. de Abreu, "Improved MDS-based multi-target tracking algorithm," in *Proc.IEEE Wireless Commun. Netw. Conf. (WCNC)*, April 2009, pp. 1800–1505.

[18] D. Macagnano and G. T. F. de Abreu, "Gershgorin analysis of random Gramian matrices with application to MDS tracking," *IEEE Trans. Signal Process.*, vol. 59, no. 4, pp. 1785–1800, 2011.

[19] A. Papoulis and S. U. Pillai, *Probability, Random Variables and Stochastic Processes*, 4th ed. New York, NY, USA: McGraw-Hill, 2002.

[20] A. J. Viterbi, *Principles of Coherent Communications*, New York, NY,USA: McGraw-Hill, 1966.

[21] G. T. F. de Abreu, "On the generation of Tikhonov variates," in *IEEE Trans. Commun.*, Jul 2008, vol. 56, p. 1157–1168.

[22] S. Severi, G. T. F. de Abreu, and D. Dardari, "Distributed localization: A comparison of performance limits," in *International Conference on Systems, Signals and Image Processing (IWSSIP)*, Apr 2012, vol. 6, p. 26–31.

[23] M. Jamalabdollahi and S. Zekavat, "ToA ranging and layer thickness computation in nonhomogeneous media," in *IEEE Trans. Geoscience and Remote Sensing*, Oct 2016, vol. 11, pp. 742–752.

[24] S. F. Chuang, W. R. Wu, and Y. T. Liu, "High-resolution AoA estimation for hybrid antenna arrays," in *IEEE Tran. Antennas and Propagation*, Apr 2015, vol. 14, pp. 2955 – 2968.

[25] B. Zhu, J. Cheng, Y. Wang, J. Yan, and J. Wang, "Three-dimensional VLC positioning based on angle difference of arrival with arbitrary tilting angle of receiver," in *IEEE J. Sel. Areas in Commun.*, Dec 2018, vol. 15, pp. 8 – 22.

[26] A. Ghods, S. Severi, G. T. F. de Abreu, S. V. de Velde, and H. Steendam, "On the structural nature of cooperation in distributed network localization," in *Asilomar Conference on Signals, Systems and Computers*, Nov 2014, vol. 5, p. 1194 – 1198.

[27] G. Shabat and A. Averbuch, "Interest zone matrix approximation," *Electronic journal of Linear Algebra*, vol. 23(1), 2012.